Simulation of Construction Process and stability analysis of surrounding rocks at the underground waterway tunnel based on ABAQUS

Kim Chol-Gyong[a], Ri Un-Chol[b*], Kim Dong-Song[a], Kim Jin-Hyok[a]

[a] Faculty of Hydraulics Engineering, Ham Hung University of hydraulics and power , Ham Hung , Democratic People's Republic of Korea
[b] Faculty of Mechanical Engineering, Ham Hung University of hydraulics and power ,Ham Hung , Democratic People's Republic of Korea

AUTHOR or CONNETION INFORMATION
* E-mail: riunchol@163.com

Abstract:

The construction process of the underground waterway tunnel was divided into two stages and the calculation and after treatment was carried out by using the ABAQUS element technique.

The study on the ground stress in the working area and the stability of the surrounding rocks were analyzed to improve the reliability of the initial surface stress equilibrium method.

As shown in the results, we can know the parameters of the surrounding rock material affect the development and deformation of the surrounding rocks during the construction of the underground waterway tunnel, and the different excavation processes also affect the deformation and the flow of the surrounding rocks.

Keyword: ABAQUS, Ground Stress, Stability, Construction Process, Initial index Stress Equilibrium method

0 preceding research

Generally, underground excavation should take into account the effects of stress and the non-linear action of the rock material.

From this, the initial index stress equilibrium, material nonlinearity structural model, and birth-death element method are analyzed when using the finite element method to analyze the underground water tunnel.

In literature [1], a finite element model for ANSYS work was created, and was progressed calculation and post-treatment by the using ABAQUS.

And then, the ground stress in the work area was investigated and the excavation was carried out through the fault, And to explore the reliability of the simulated method of surrounding cancer parameters.

In literature [2], researcher determined the reliability of the ABAQUS program through dynamic simulation about the stage excavation process of a large underground water tunnel by the using of ABAQUS.

In addition, there are process lipid method, the simulation experiment method, the field observation method, and the numerical analysis method in the method of studying the stability problem of the rock around the underground water.

In literature [3], the stress distribution near single layer was studied at a new viewing, and then the stability of the surrounding rocks was analyzed and the adverse effect of the material parameters on the stability was derived.

In literature [4], numerical simulations of the stability of the surrounding rocks under the influence of the single layer were carried out.

In literature [4], a study was conducted on the stability of the rock around the water tunnel in the geotechnical stress measurement direction.

From the reviewing of the combination of the preceding documents shows that the construction process of the underground water tunnel and the material parameters of the surrounding rocks play an important role in stability and a deep research are needed.

1. Status and geological condition

The Erangcheon Hydroelectric Power Station is the third power plant developed in terraced form at Erangcheon Station in Erang-town. When the sea surface elevation is 2780m, Watershed area is 2453 m^2, average annual flow rate is 132 m^3/s, power plant capacity is 9600kW and average annual power generation is 6714,000kWh.

Waterproof structures mainly include spillway and waterproof water tunnel.

The total length of the waterproof tunnel is 536.66m and it is a molding oyster and it is installed in the left sliding surface.

The rock body components of the tunnels 0 + 080 ~ 0 + 395 of the banishment

Water tunnel are hornblende, and weak efflorescence-micro efflorescence rocks are basic.

According to Annex J of the "Hydrographic Observation Standards for Geological Observations", if the surrounding rocks are classified according to the criteria, they belong to Class III rocks.

On the up of the water tunnel is covered that with rock whose thickness is five times the average diameter of the water tunnel diameter pole. It belongs to class IV rock.

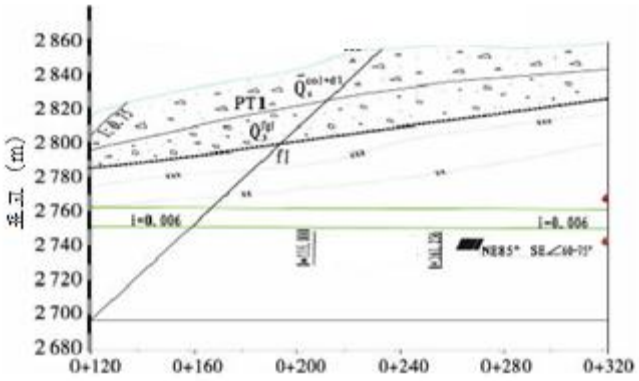

Figure1. Water tunnel cross section

2. Numerical analysis

2.1 Assumptions

Underground excavation calculations often take into account the impact of surface stresses.

The analysis of surface stress equilibrium is required because the deformation does not occur in the underground water column before excavation.

This gives the initial stress field, which is based on the following assumptions.

1) The initial stress field only considers gravity action.

2) We do not consider the effect of excavation process of groundwater.

3) The construction process simulation is regarded as a secondary excavation process.

4) The surrounding rocks are not uniformly distributed.

2.2 Calculation model and calculation parameters

Create a model using ABAQUS / CAE.

Part-1 is a rock with a square of 200 × 200m square, with a 30m × 20m rectangular quadrangle in the middle and a 15m-radius semicircle with a radius of 15m.

It creates an underground water boulder, Part-2, which is in contact with an underground waterfall.

Before the excavation, the surrounding rock body and the underground water glaciation body are all integrated.

However, when creating a model according to the method described in the right, the finite elements of the two partial arm bodies are separated on the tangent interface.

In other words, there are two nodal points at the same position on the tangent boundary.

In order to reasonably simulate the situation before the excavation, proceed to establish the Tie bondage for the two parts Part-1 and Part-2.

The material parameters are obtained from the topography data of the Erangcheon hydroelectric power plant and are shown in Table 1.

Table 1. Material parameter

Type	Density ρ/ (kg•m^{-3})	Elasticity variable E/GPa	μ	Pulling resistance strength R/MPa	Cohesion c/MPa	Friction angle ψ/°
Ⅲ type rock	2650	8	0.25	2.2	1.0	45
Ⅳ type rock	2450	5	0.3	2	0.5	36
Concrete (C40)	2400	32.5	0.2	1.71		

3. Initial Stress Field Analysis

The initial stress field is applied to the model in order to guarantee the initial displacement, and it must be balanced with the ground stress.

In other words, the stress is taken as the proof force through the calculation, and the gravity load is applied again to make the equilibrium.

This initial stress period is realized and at the same time, the initial displacement is ensured by the command. There are four methods for balancing the ground stress of ABAQUS.

That is, there are a method of taking initial stress, a method of defining clue, a method of defining a partial program, and an (AUTO-BALANCE) automatic balancing method.

In this case, soil stress equilibrium is preceded by using initial stress taking into account the unevenness of the ground surface and unevenness of the clay material.

This method can be realized by using the file FILENAME.INP.

First, the boundary condition is given to the model and the calculation is performed. Then, the stress of the intermediate element obtained by the calculation is extrapolated up to the core point, and then the six stress amounts are derived.

The obtained stress is applied to the model with the proof force and the calculation is carried out again by applying a gravity load.

This realizes the soil stress equilibrium and keeps it with the name "exca_equiv.inp". (Here, the displacement unit is m and the stress unit is Pa.

Figure 2 shows the comparison between the results of considering the initial surface stress balance and the results without considering the surface stress balance.

As can be seen in the figure, both the median stress amount and the maximum minimum principal stress after the initial surface stress balance are basically consistent with the self-weight stress.

In addition, the displacement magnitude changes from 10^{-7} on the Cm scale in self-weight. That is, it approaches the command. Thus, the requirement for the surface stress balance is satisfied.

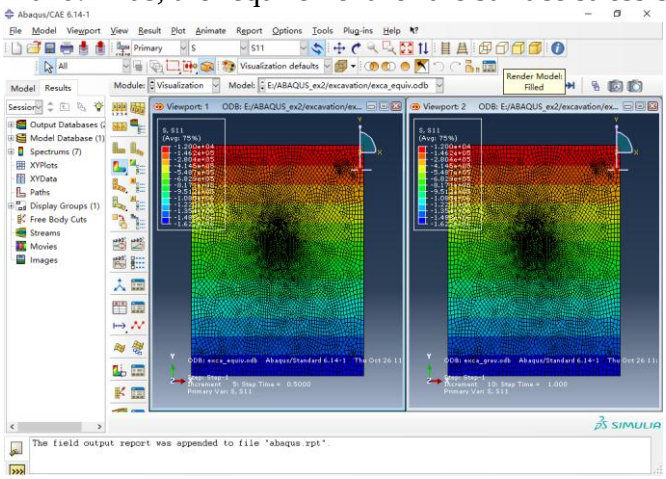

Figure 2. Results after surface stress balance (S11 stress comparison)

4. Stability analysis of underground water rocks and surrounding rocks

4.1 Analysis of the effect of excavation process on stability of the water

The excavation of underground watercourses is carried out by using birth-death element method.

In the file "exca_equiv.inp" of the Inp file of the surface stress balance calculation, proceed with the correction.

The underground watercourse is divided into two upper and lower layers, but only after completing the self-weighted surface stress balance, two analysis steps are attached.

Use the clue "Model Change, Remove" to remove the excavated element meeting.

To emphasize the nonlinear sexuality based on the calculation, activate the parameter "UNSYMM = YES" in "* Step" and then use the asymmetric matrix savings to obtain the solution "* CONTROLS, ANALYSIS = DISCONTINUOUS" can do. Save the Inp file with another name "exca_std.inp".

The first excavation analysis is carried out together to study the effect of the excavation process.

To do this, remove the entire underground gangway body from this analysis block and save the Inp file as "exca_red_tc_o.inp".

Figure 3 compares the results of the first excavation and the second excavation.

Here, the plastic deformation zone of the primary excavation is small and the range of the equivalent plastic deformation distribution is smaller than that of the layer excavation.

Likewise, the equivalent pull-out stress and Mises stress are relatively small. The displacement distribution is basically consistent, but the primary excavation situation is smaller in number value.

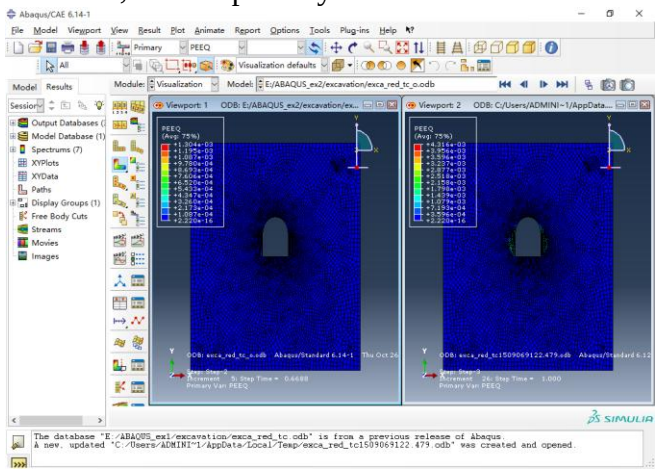

(a)

Figure 3. Comparison of primary excavation and fractional excavation results (friction angle 36 °, cohesion strength 0.5Mpa, Cut resistance pull strength 0.1Mpa)

(a) Equivalent plastic stress strain distribution

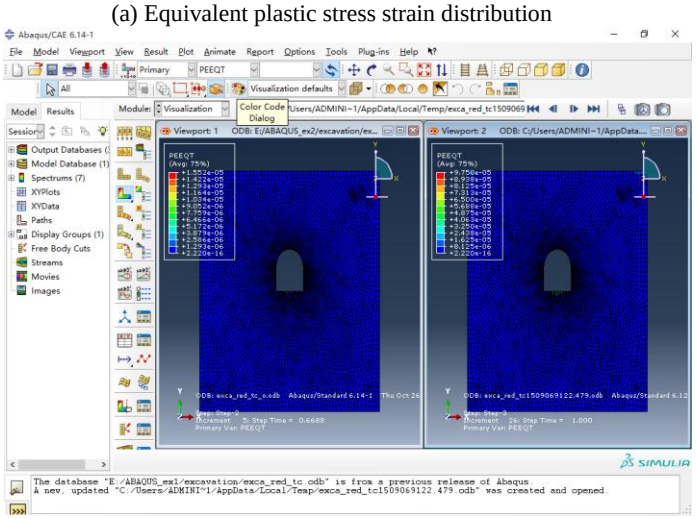

(b)

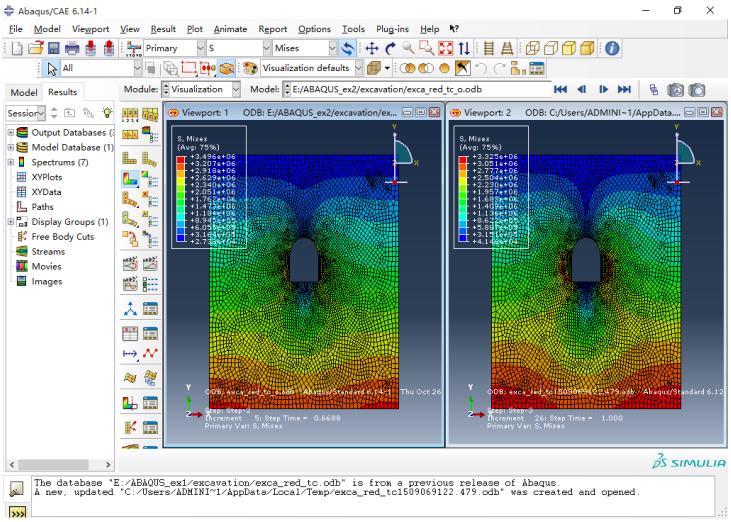

(c)

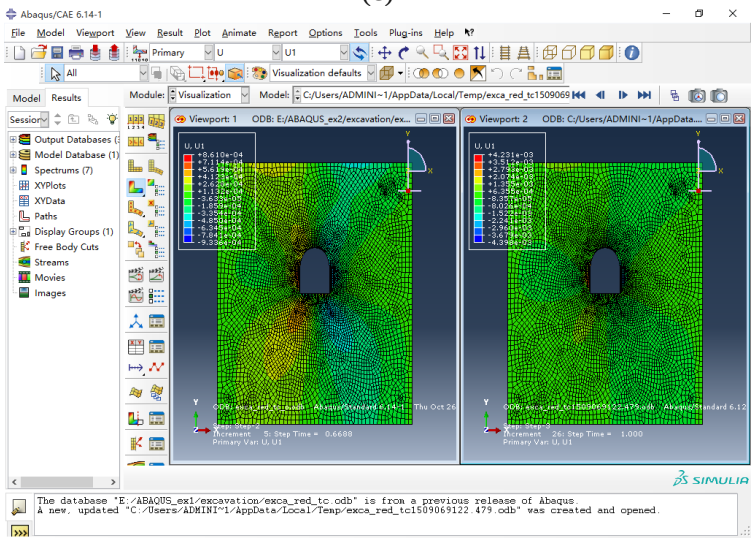

(d)

Figure 3. Comparison of primary excavation and fractional excavation results (friction angle 36 °, cohesion strength 0.5 Mpa, Cut resistance pull strength 0.1 Mpa)(b) Equivalent pulling-plastic stress strain distribution; (c) Mises stress distribution; (d) Horizontal displacement distribution

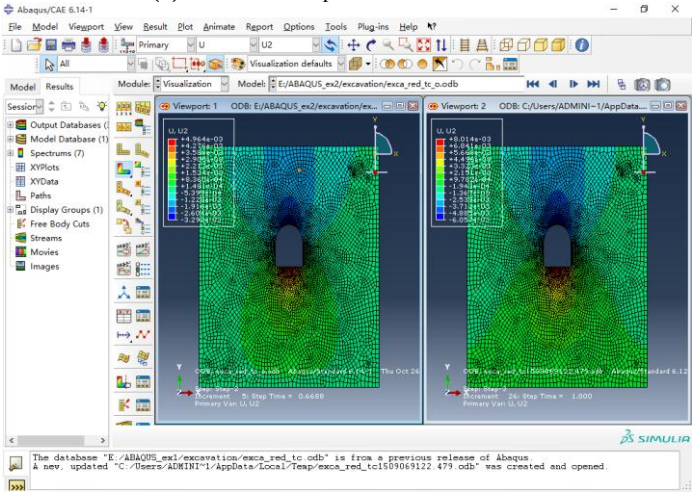

(e)

Figure 3. Comparison of primary excavation and fractional excavation results (friction angle 36 °, cohesion strength 0.5 Mpa, Cut resistance pull strength 0.1 Mpa)
(e) Vertical displacement distribution

4.2 Analysis of the effect of material parameters on the stability of surrounding rocks

4.2.1 Case where the rock friction angle is 45 ° and the cohesive strength is 1.0Mpa (Ⅲ type rock)

Edit the archived Inp file "exca_std.inp" and proceed with the calculation.

The calculation results are shown in Fig. 4 and Fig. 5, which show the Mises stress, vertical and horizontal displacements, and equivalent plastic stress distributions of the surrounding rock masses, respectively, after the water excavation and lower excavation.

As can be seen in the figure, the surrounding rocks are only plastic deformation (yielding, floating) at the edge wall of the excavation floor under the condition of 45 °of arm friction angle and 1.0Mpa of cohesion strength.

Horizontal displacement toward the inside of the water tunnel occurs on the wall of the left and right side of the water tunnel, and the size is about 0.1 cm.

0.7 cm rightward displacement occurs at the gill bottom and a 0.5 cm downward displacement occurs at the tunnel action point.

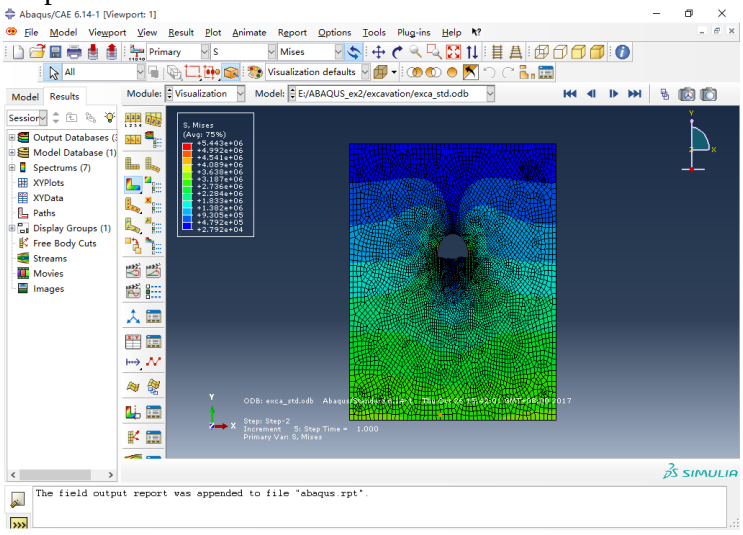

(a)

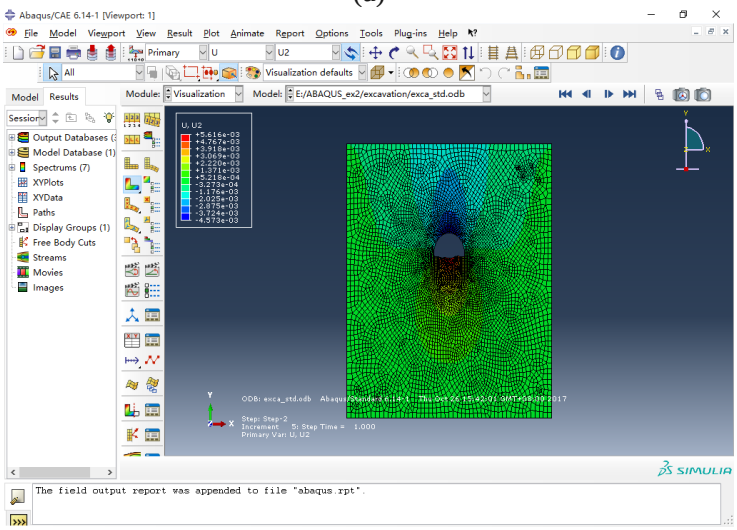

(b)

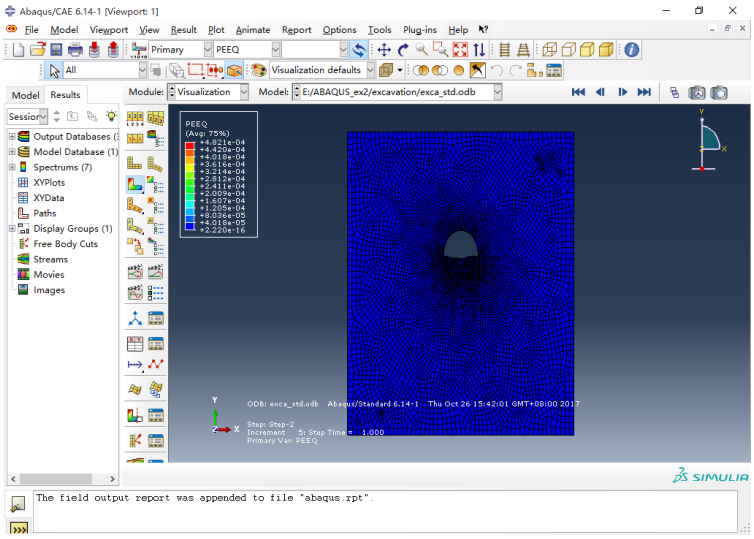

(c)

Figure 4. Result after upper excavation (45 °of friction angle, cohesion strength of 1.0 MPa)
(a) Mises stress distribution, (b) vertical displacement distribution; (c) Equivalent plastic stress strain distribution

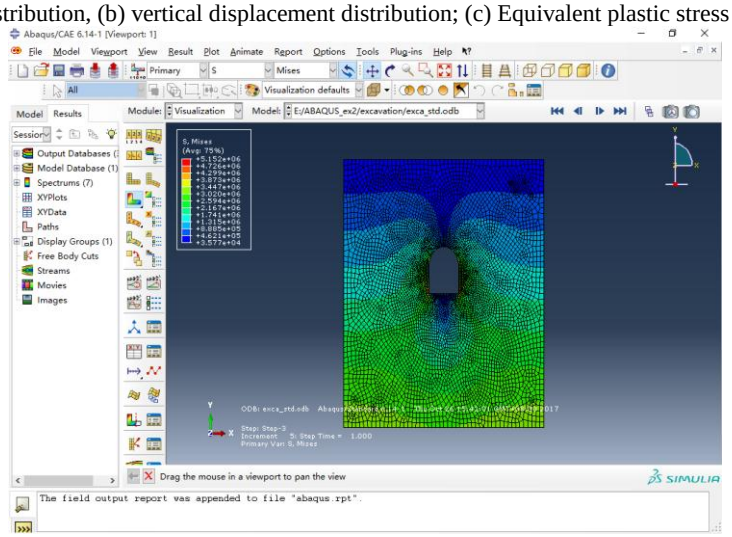

(a)

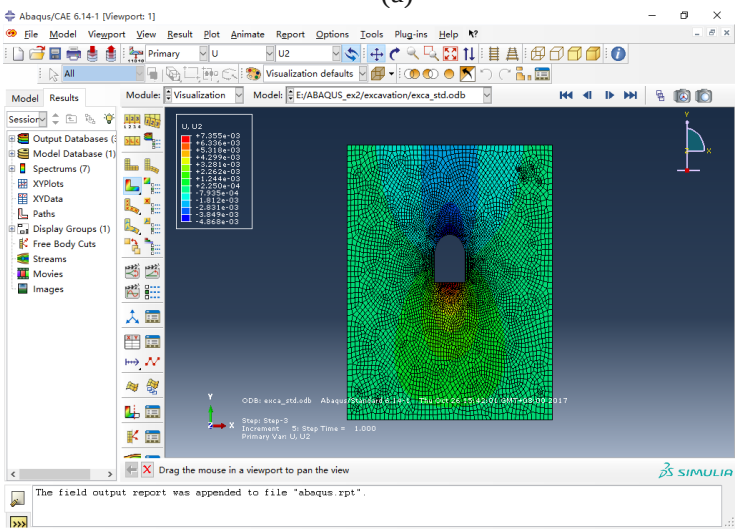

(b)

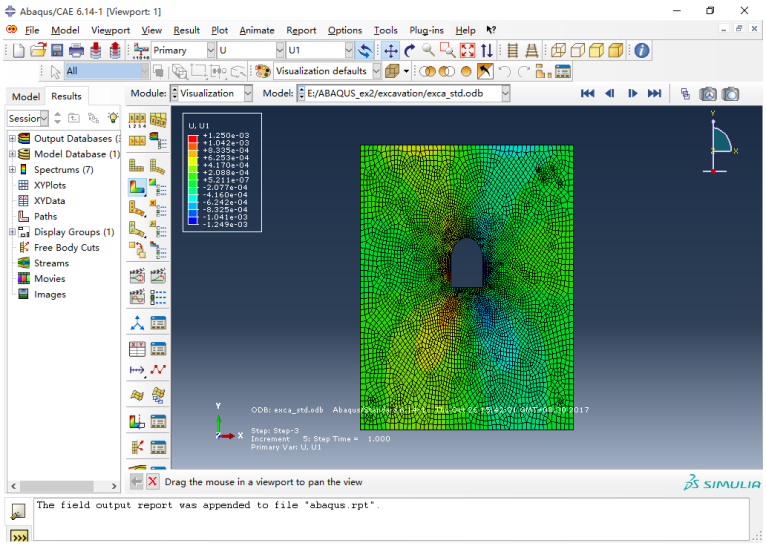

(c)

Figure 5. Result after under-floor excavation (friction angle 45 °, cohesion strength 1.0MPa)
(a) Mises stress distribution; (b) vertical displacement distribution; (c) Horizontal Displacement Distribution

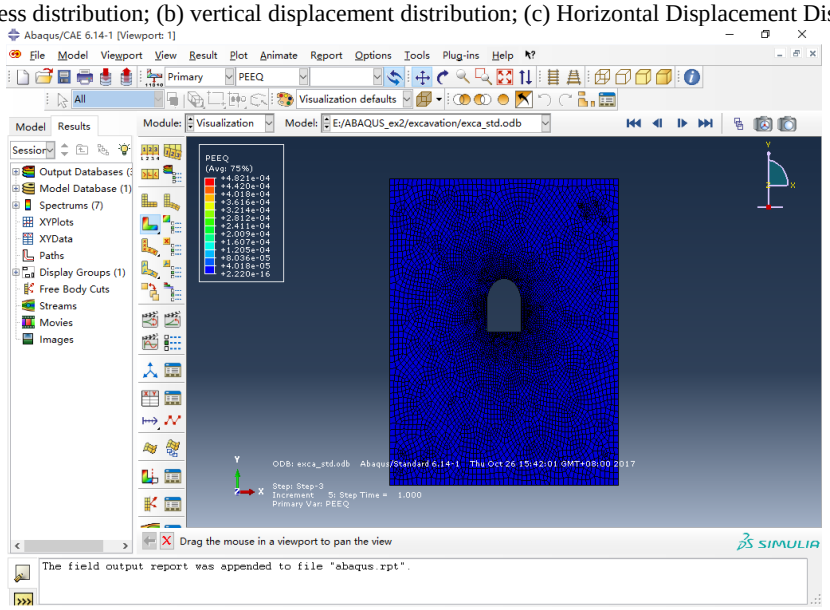

(d)

Figure 5. Result after lower excavation (friction angle 45 °, cohesion strength 1.0MPa) (consecutive)
(d) Equivalent plastic stress strain distribution

4.2.2 When the rocky body's friction angle is 36 ° and the cohesion strength is 0.5Mpa (Ⅳ type rock)

Take the surrounding rocks as the class IV rock. That is, take a friction angle of 36 ° and a cohesive strength of 0.5Mpa and proceed with the corresponding material parameter modification and then store the Inp file as "exca_red.inp". The calculation results are shown in Fig. 5 and Fig. 6.

As can be seen from the Mises stress distribution, there is a circular arc high stress zone from the gill bottom to the left and right frame walls, which may be a plastic deformation zone. As shown in the equivalent plastic stress distribution map, two concentrated plastic deformation bands are generated on the left and right edge walls of the gantry. Left and right border walls Horizontal displacement is about 0.4cm, the displacement towards the right is 0.8cm, and the ceiling is downward 0.6cm.

The material properties in the Inp file are defined by considering that the trimming resistance pulling strength of the more-clone model is 0.1Mpa. To do this, attach a cliche "* Tensile Cutoff" and take the data line as "100000, 0" and keep the Inp file as "exca_red_tc.inp". To investigate the effect of considering the trimming resistance pulling force, the morph on parameter is set at a friction angle of 36 ° and a cohesive strength of 0.5Mpa. Calculation result Mises Stress, displacement, and equivalent plastic strain Stress distribution on the size and size, but the plastic

deformation at the bottom of the gin bottom after excavation can occur when the trimming resistance strength is taken into consideration.

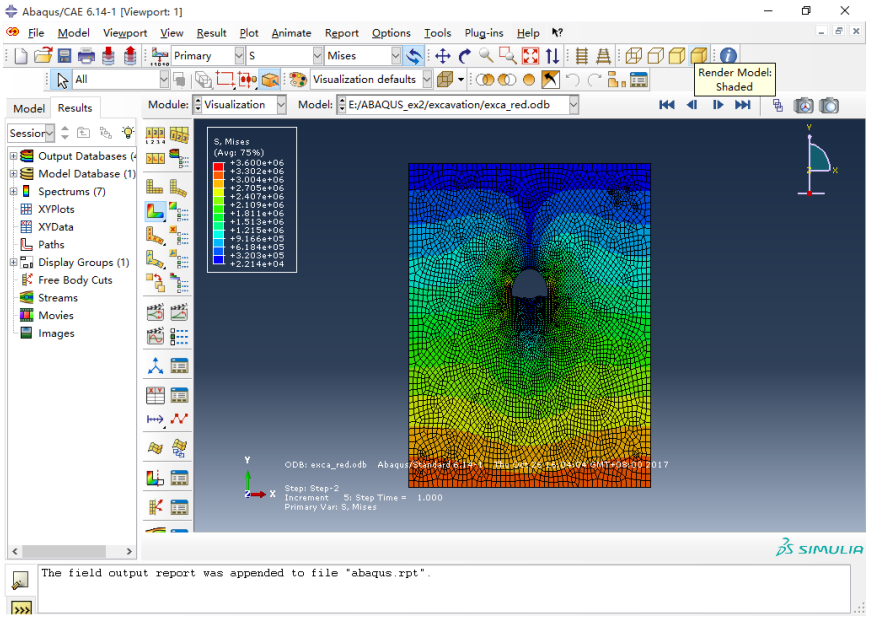

(a)

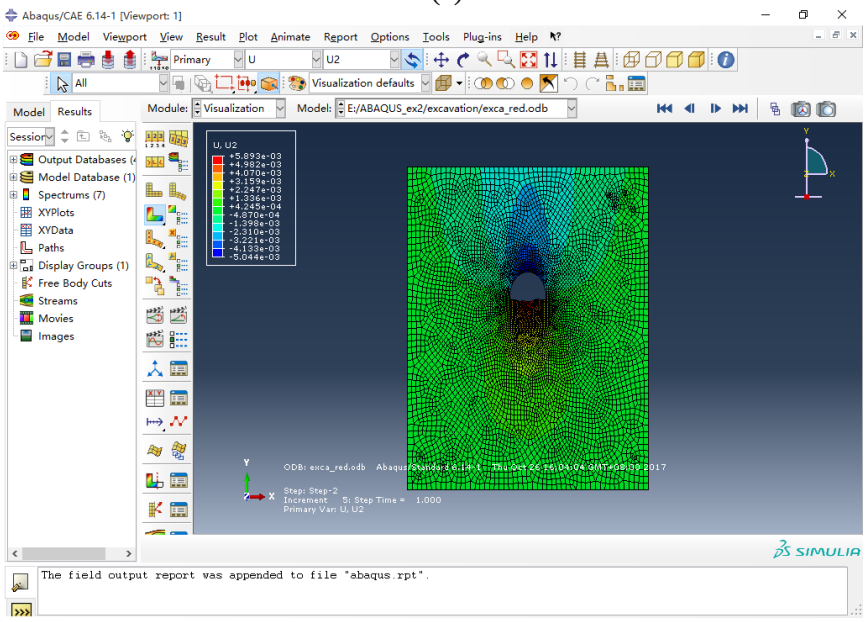

(b)

Figure 6. Result after upper excavation (friction angle 36 °, cohesion strength 0.5 MPa)
(a) Mises stress distribution; (b) Vertical displacement distribution

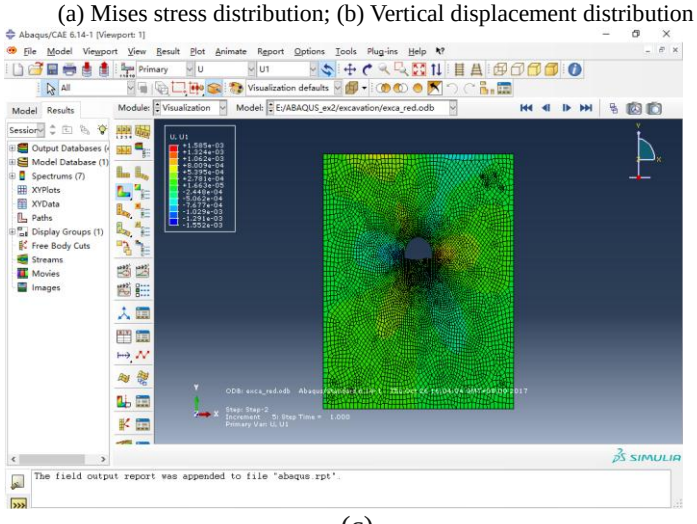

(c)

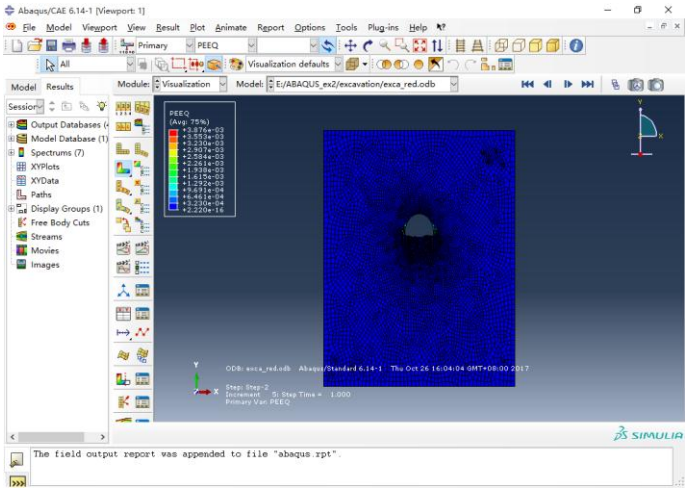

(d)

(a) Figure 6. Result after upper excavation (friction angle 36 °, cohesion strength 0.5MPa) (consecutive)
(c) Horizontal displacement distribution; (d) equivalent plastic stress strain distribution

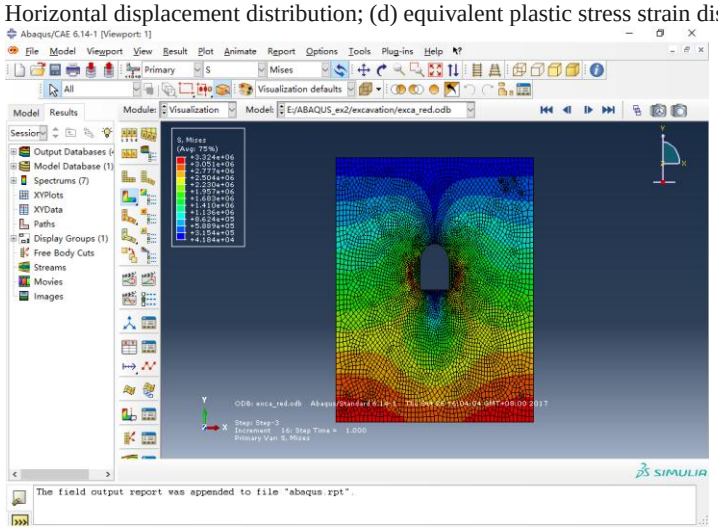

(a)

Figure 7. Results after lower excavation (friction angle 36 °, cohesion strength 0.5MPa)
(a) Mises stress distribution

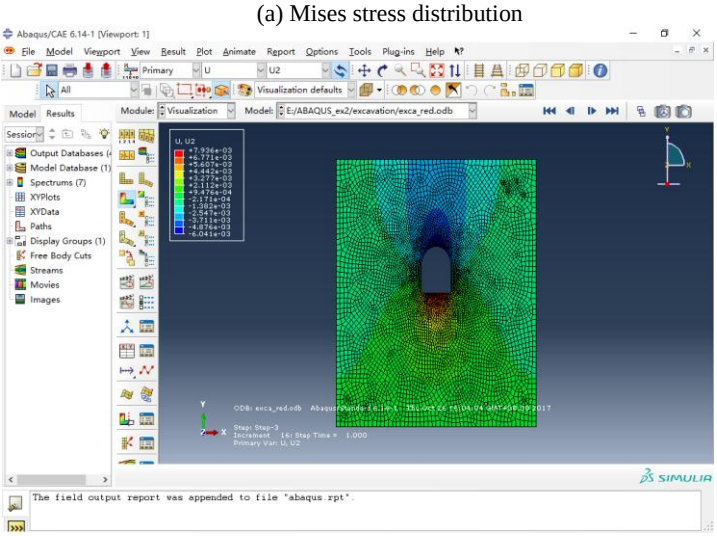

(b)

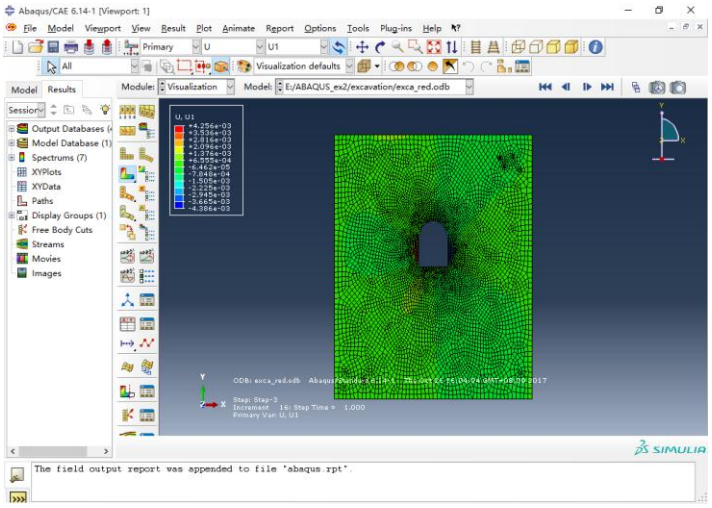

(c)

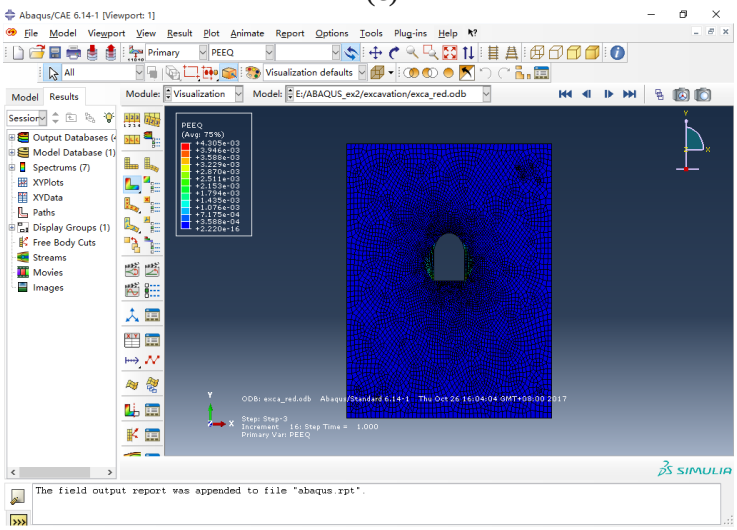

(d)

Figure 7. Result after lower excavation (friction angle 36 °, cohesion strength 0.5MPa) (consecutive)
(b) Vertical displacement distribution; (c) horizontal displacement distribution;
(d) equivalent plastic stress strain distribution

5. Conclusion

In this study, the stability of the surrounding rocks according to the parameters and the parameters of the underground water ponds were analyzed by using ABAQUS 's initial surface stress balance method, urea technique, Tie bond, and mor - clone model.

In this process, the influence of the morphologic model parameters on the development and deformation of the surrounding plastic deformation zone was analyzed.

At the same time, the effects of various excavation processes on the surrounding rock deformation and plastic deformation were analyzed.

The following conclusions were obtained.

1) If there are two nodal points at the same position on the tangent boundary, it is useful to proceed with the tie bond establishment in order to reasonably simulate the situation before the excavation.

2) Under the assumption that self-weight is a fundamental factor of the initial stress field, it is most effective and possible to use the initial stress search method for the surface undulation situation.

3) As a result of the comparison between the first excavation and the layer excavation, the plastic deformation zone of the first excavation is small and the range of equivalent plastic deformation is smaller than that of the conventional excavation. And the equivalent pulling plastic stress and Mises stress are relatively small in the first excavation and the displacement distribution is basically the same in both cases, but the first excavation situation is smaller in number value.

4) Calculation result according to the material parameters of the surrounding rocks. Horizontal displacements toward the inside of the water tunnel occur on the walls of the left and right sides of the water tunnel, and downward displacement occurs on the bottom of the water tunnel. Its size increases as the rock mass decreases in strength.

References:

[1] 都辉,任旭华, 张继勋. 基于ＡＢＡＱＵＳ的地下隧洞开挖及围岩稳定性分析［Ｊ］. 三峡大学学报（自然科学版），2014, 36 (2)：28－32.

[2] 陈浩，肖明，衡为方. 基于ＡＢＡＱＵＳ大型地下洞室群分期开挖动态模拟［J]. 武汉大学学报（工学版), 2013, 46 （３）：321－327.

[3] 邓声君，陆晓敏，黄晓阳. 地下洞室围岩稳定性分析方法简述［Ｊ］. 地质与勘探，2013, 49(3)：541－547.

[4] 阮彦晟. 断层附近应力分布的异常和对地下工程围岩稳定的影响［Ｄ］. 济南：山东大学，2008.

[5] 崔 芳, 高永涛，吴顺川. 断层影响下隧道围岩稳定性的数值分析[Ｊ]. 公路，2011(9) :242-245.

[6] 吴满路，廖椿庭. 大茅隧道地应力测量及围岩体稳定性研究［Ｊ］. 地质力学学报，2000, 6(2)：71-76.

[7] 代汝林, 李忠芳, 王 姣. 基于ＡＢＡＱＵＳ的初始地应力平衡方法研究 ［Ｊ］. 重庆工商大学学报：自然科学版，2012, 29(9)：76-81.

[8] 晁建伟，余同勇，韦四江. 回采巷道过断层顶板破坏特征研究［Ｊ］. 矿业安全与环保，2009, 36(2)：13-15.

[9] 付存仓，温 森. 断层对巷道附近塑性区的影响［Ｊ］. 采矿技术，2006, 6(2)：31-32.

[10] 刘 学. 采用 ＡＢＡＱＵＳ的隧道稳定性分析［Ｊ］. 山西建筑，2009, 35(9)：312-313.

[11] 冯夏庭，张传庆，李邵军，等. 深埋硬岩隧洞动态设计方法［M]. 北京：科学出版社，2013：354-356.